Journal of Non-Newtonian Fluid Mechanics, 50 (1993) 305–329
Elsevier Science Publishers B.V., Amsterdam

Anomalous rolling of spheres down an inclined plane

Y.J. Liu, J. Nelson, J. Feng and D.D. Joseph *

Department of Aerospace Engineering and Mechanics, University of Minnesota, 107 Akerman Hall, 110 Union Street SE, Minneapolis, MN 55455 (USA)

(Received June 21, 1993)

Abstract

A sphere in air will roll down a plane that is tilted away from the vertical. The only couple acting about the point of contact between the sphere and the plane is due to the component of the weight of the sphere along the plane, provided that air friction is negligible. If on the other hand the sphere is immersed in a liquid, hydrodynamic forces will enter into the couples that turn the sphere, and the rotation of the sphere can be anomalous, i.e., as if rolling up the plane while it falls. In this paper we shall show that anomalous rolling is a characteristic phenomenon that can be observed in every viscoelastic liquid tested so far. Anomalous rolling is normal for hydrodynamically levitated spheres, both in Newtonian and viscoelastic liquids. Normal and anomalous rolling are different names for dry and hydrodynamic rolling. Spheres dropped at a vertical wall in Newtonian liquids are forced into anomalous rotation and are pushed away from the wall while in viscoelastic liquids, they are forced into anomalous rotation, but are pushed toward the wall. If the wall is inclined and the fluid is Newtonian, the spheres will rotate normally for dry rolling, but the same spheres rotate anomalously in viscoelastic liquids when the angle of inclination from the vertical is less than some critical value. The hydrodynamic mechanisms underway in the settling of circular particles in a Newtonian fluid at a vertical wall are revealed by an exact numerical simulation based on a finite-element solution of the Navier-Stokes equations and Newton's equations of motion for a rigid body.

Keywords: anomalous (or hydrodynamic) rolling; Newtonian liquids; normal (or dry) rolling; numerical simulation; settling of spheres; viscoelastic liquids

* Corresponding author.

1. Introduction

Goldman et al. [1] treated the problem of interaction between a sphere and a wall. They also considered the problem of a sphere "rolling" down an inclined wall and found that the sphere cannot be in physical contact with the wall and that it slips, giving rise to anomalous rotation when forced into close approach. In this paper "anomalous" is defined as the sense of rotation that exists when the sphere rotates as if it were rolling up the wall. We define "normal" rotation as the sense of rotation that occurs when the sphere rotates as if it were rolling down the wall. Bungay and Brenner [2] showed that the rotation of a tightly fitting ball falling down a vertical tube would change sense, from anomalous to normal, as the distance between the ball and the tube wall tended to zero. The Stokes flow predictions of these authors involve neither inertia nor elasticity. The phenomenon of anomalous rolling that they predicted appears in the experiments of Humphrey and Murata [3], who found that the rotation of a sphere gradually changes from anomalous to normal as the tube inclination angle is increased and the sphere contacts the wall. They think that inertia-induced lift keeps the rolling ball off the wall at the smaller angles of inclination.

Dhahir and Walters [4] studied flow past a cylinder in a straight channel of rectangular cross-section. They did experiments with Newtonian fluids, 2% and 3% Xanthan (Kelco) in water, and 1.5% aqueous polyacrylamide (an elastic fluid). Looking at a horizontal Poiseuille flow moving from left to right, with a cylinder above the center line, the cylinder will rotate against the clock as if turned by shears from the center part of the channel rather than from the gap between the cylinder and the wall. For all of the non-Newtonian fluids, the flow generated a side force that pushed the cylinder toward the wall, no matter where the cylinder was placed. This side force was too small to measure in Newtonian liquids. These results are totally consistent with phenomena we have observed on the lateral motions of spheres settling along a wall.

Jones and Walters [5] did experiments on the flow of polymeric liquids through a channel blocked by a periodic array of staggered cylinders, simulating a porous medium. They found that the elastic polyacrylamide did not easily pass through the narrow passage between the channel wall and the cylinder, but the Newtonian liquids and aqueous Xanthan were not blocked. Blockage, even partial blockage, can produce a situation in which a cylinder or sphere is turned by the shears from the fluid that goes around the outside of a sphere, leading to the rolling that we have called anomalous, but that is normal when the turning is controlled by hydrodynamics (see Fig. 1). A mechanistic description of the hydrodynamics

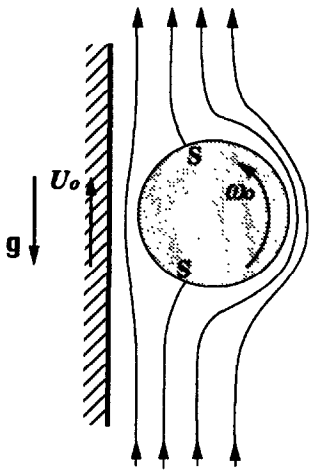

Fig. 1. Cartoon of the settling of a circular particle at a vertical wall in a coordinate system in which the center of the particle is at rest, so the wall moves up with speed U_0. If the particle is dropped at the wall, the fluid will go around the outside and turn the particle in the anomalous sense as shown. There are two "stagnation" points S on the circle where the shear stress vanishes (see Section 5 for a precise description) associated with high positive pressure on the bottom and a smaller negative pressure near the top. The positive pressure "lifts" the particle away from the wall and it seeks an equilibrium in the channel center. The cartoon is based on a two-dimensional simulation whose relation to the experiments is apparent but not fully clarified.

underway for the rotations induced by the settling of a circular particle in two dimensions will be presented in Section 5, but an understanding of the fluid mechanics underway in the viscoelastic case has yet to be revealed.

Joseph et al. [6] found anomalous rolling of a sphere along an inclined wall. The angle between the wall and gravity was varied so that the sphere fell on, rather than away from, the wall. A sphere falling down these inclined walls rotated normally in viscous liquids as it does in dry rolling, but rotated anomalously in the other sense in viscoelastic liquids when the wall was not tilted too far from the vertical. In this paper we document this phenomenon by reporting observations and measured data for many different polymeric liquids. We find anomalous rolling in all liquids, Newtonian and viscoelastic, when the wall is vertical, even though spheres are repelled by the wall in Newtonian liquids and attracted to the wall in viscoelastic liquids. The anomalous results for rolling spheres in apparent (only) contact with tilted walls are as reported by Joseph et al. [6] with the caveat that viscoelastic solutions with weak or no normal stresses stand between Newtonian and viscoelastic behavior.

TABLE 1

Material parameters of fluids used in experiments; percentages are by weight

Fluid	ρ (g cm^{-3})	η_0 (Pa.s)	k	n	$\hat{\beta}$ (g cm^{-1})	n_1 (g cm^{-1})	c (cm s^{-1})	λ_0 (s)
1.5% aqueous polyox	1.00	20.4	10.1	0.38	132	440	20.3	0.495
1.25% aqueous polyox	1.00	11.2	6.42	0.39	117	389	17.2	0.378
1.0% aqueous polyox	1.00	7.65	3.97	0.42	108	360	15.0	0.34
0.4% Carbopol in 50/50 glycerin–water	1.13	0.76	0.31	0.67	0	0	15.9	0.027
0.3% aqueous Xanthan	1.00	5.21	1.1	0.28	0	0	12.2	0.35
S1	0.875	8.06	7.14	0.62	11.8	39.3	72.4	0.018
STP	0.86	18.0	17.8	0.85	0.97	3.23	286	0.0026

Experiments were also done in more dilute polyox solutions (WSR 301) and in a 1.2% polyacrylamide solution in a 50/50 glycerin–water solution, but the material parameters were not measured. The numerical value k is the value of the viscosity in Pa.s at a shear rate $\dot{\gamma} = 1$. The relaxation time $\lambda_0 = \eta_0/\rho c^2$.

2. Material and dimensionless parameters

The material parameters (Table 1) that were measured in the liquids used in the experiments are the density ρ, viscosity $\eta = k\dot{\gamma}^{n-1}$, where $\dot{\gamma}$ is the shear rate in reciprocal seconds, the climbing constant $\hat{\beta}$ measured on a rotating rod viscometer (Beavers and Joseph [7]) and the wave speed c. To compute $\hat{\beta}$ from measured values of the climb, we need the interfacial tension which we measured with a spinning drop tensiometer (Joseph et al. [8]). The value of $\hat{\beta}$ is insensitive to a small change of surface tension (Chapter 16 in Joseph [9]).

The climbing constant $\hat{\beta}$ is related to the limiting (zero shear) value of the first and second normal stress differences

$$(n_1, n_2) = \lim_{\dot{\gamma}\to 0} (N_1(\dot{\gamma}), N_2(\dot{\gamma})]/\dot{\gamma}^2 \tag{2.1}$$

by

$$\hat{\beta} = \tfrac{1}{2}n_1 + n_2. \tag{2.2}$$

The climbing constant

$$\hat{\beta} = 3\alpha_1 + 2\alpha_2 \tag{2.3}$$

may also be expressed in terms of quadratic constants

$$(\alpha_1, \alpha_2) = (-\tfrac{1}{2}n_1, n_1 + n_2) \tag{2.4}$$

of the second order fluid. $\alpha_2/|\alpha_1|$ is the ratio of quadratic constants and

$$[\alpha_1, \alpha_2] = [-m, 2m - 2]\hat{\beta}/(m - 4), \tag{2.5}$$

where $m = 2\alpha_1/(2\alpha_1 + \alpha_2) = -n_1/n_2$ is the ratio of the first to second normal stress differences. It can be argued (Section 17.11 in Ref. 9) that $m = 10$ is a reasonable value for our polymer solutions. Then

$$\frac{\alpha_2}{|\alpha_1|} = \left|\frac{2(1-m)}{m}\right| = 1.8 \tag{2.6}$$

is constant and α_1 and α_2 are determined by the measured values of the climbing constant $\hat{\beta}$. The value of n_1 we get from measuring $\hat{\beta}$ is not sensitive to the value of the ratio n_2/n_1 as long as n_2 is relatively small and negative.

The measured value of the climbing constant, together with the assumption that the second normal stress difference is $-1/10$ as large as the first, allows us to evaluate Roscoe's [10] formula

$$T_{11} - T_{22} = 3\dot{s}\eta_0 + 3(\alpha_1 + \alpha_2)\dot{s}^2 \tag{2.7}$$

for the extensional stress difference where $\dot{s}$ is the rate of stretching in the direction x_1 and η_0 is the zero shear viscosity. Using (2.6) and $\alpha_1 = -n_1/2$ we get

$$T_{11} - T_{22} = 3\dot{s}\eta_0 + 1.2n_1\dot{s}^2. \tag{2.8}$$

The zero shear value of the first normal stress difference $n_1 = (2m/(m-4))\hat{\beta} = 10/3\hat{\beta}$ and the zero shear quadratic correction $4\dot{s}\hat{\beta}$ of Trouton's viscosity, $3\eta_0$, increase with $\hat{\beta}$. An argument given by Liu and Joseph [11] suggests that extensional stresses, broadly speaking, control the properties of the aggregation of particles in viscoelastic liquids documented here.

Glycerin and water mixtures in various concentrations were used to determine Newtonian behavior. The polyox and polyacrylamide solutions are standard test viscoelastic liquids exhibiting normal stresses, shear thinning and memory effects.

STP is a solution of polyisobutylene (PIB) in petroleum oil that was used extensively in early studies of rod climbing [9]. S1 is a solution of 50.0 g of 5% (w/w) of PIB in decalin plus 5% polybutene oil, a world-wide standard test fluid that is being characterized by different laboratories in many countries. We mixed our own samples according to procedures laid down by Professor J. Ferguson of the University of Glasgow. Our homemade solutions have nearly the same properties as the premixed samples given to us.

The viscosity of these two polymer solutions, measured as a function of the shear rate $\dot{\gamma}$ on the RSF2 Rheometrics fluid rheometer is given in Fig. 2. The viscosity of STP is nearly constant for shear rates less than 100. The viscosity of S1 decreases with increasing $\dot{\gamma}$, but the decrease is very slow for shear rates less than 10. The viscosity of S1 is an order of magnitude smaller than STP; it is a much more mobile liquid. Both solutions climb a rotating rod, but the STP is not a good climber; the climbing constant at room

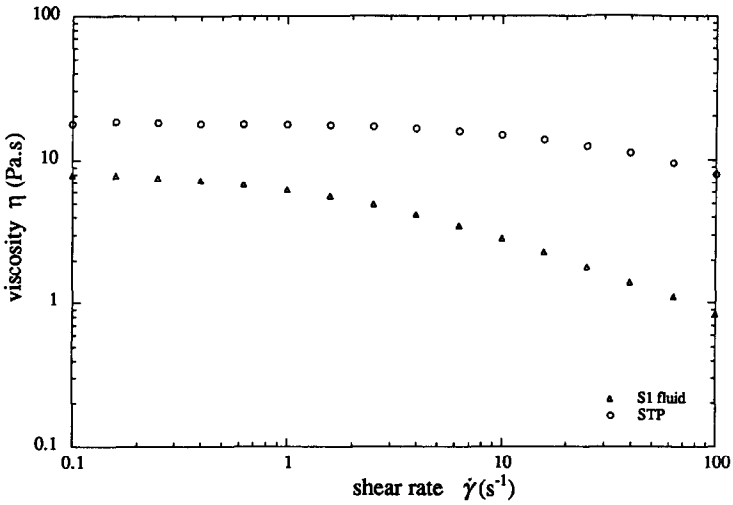

Fig. 2. The viscosities of STP and S1 fluids as functions of the shear rate measured, at a temperature of 24.5°C, on a RSF2 Rheometrics fluid rheometer with a cone of 50 mm diameter and 0.021 radian cone angle and a plate. The viscosity of S1 is an order of magnitude smaller than STP; it is a much more mobile liquid. S1 has a small shear thinning, and STP is more like a Boger fluid. The power law constants for S1, for shear rates greater than 0.5 s^{-1}, are $\kappa = 7.14$ and $n = 0.62$, whereas for STP, $\kappa = 18.7$, $n = 0.85$.

temperature is about 1 g cm^{-1}. We can say that STP is a Boger fluid with very weak normal stresses. The climbing constant of S1 at 25°C is approximately 11.8 g cm^{-1} and S1 can be said to resemble STP with much larger normal stresses, especially at low rates of shear.

Values for the dynamic moduli of STP and S1 are given in Fig. 3. The loss modulus for STP is an order of magnitude higher than that for S1. The storage modulus of S1 is larger than for STP for shear rates less than about 10 s^{-1}, and the shear rate at which the loss modulus falls below the storage modulus is much lower in S1 than in STP. S1 is more mobile and much more elastic liquid than STP.

We attempted to isolate the role of shear thinning, suppressing both normal stresses and elasticity, by using a solution of 0.4% Carbopol 690 (Goodrich) in a 50/50 glycerin–water mixture in our sedimentation experiments. The viscosity vs shear rate for this Carbopol solution is plotted in Fig. 4, and the dynamic moduli are plotted in Fig. 5. Carbopol is thought to be a pseudoplastic fluid without elasticity. Since our Carbopol solution has a non-zero storage modulus, it cannot be said to be without elasticity. The presence of small elasticity in Carbopol solutions has been noted before; for example, Hartnett and Kostic [12] have noted that an aqueous solution of 1000 ppm (by wt.) Carbopol exhibits elasticity in the linear

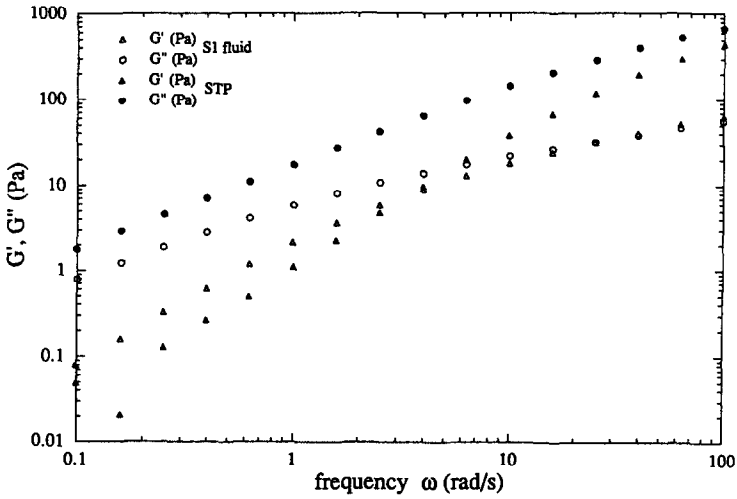

Fig. 3. Dynamic moduli of STP and S1 measured, at 2% strain, on the same rheometer with the same pair of cone and plate as in Fig. 2. The loss modulus for STP is an order of magnitude higher than for S1. The storage modulus of S1 is larger than for STP for shear rates less than about 10. The shear rate at which the loss modulus falls below the storage modulus for S1 is much lower than that for STP.

viscoelastic regime, and found evidence that aqueous Carbopol solutions experience strong secondary motions in laminar flow in non-circular channels, but they do not reduce drag. There is no evidence that Carbopol 690

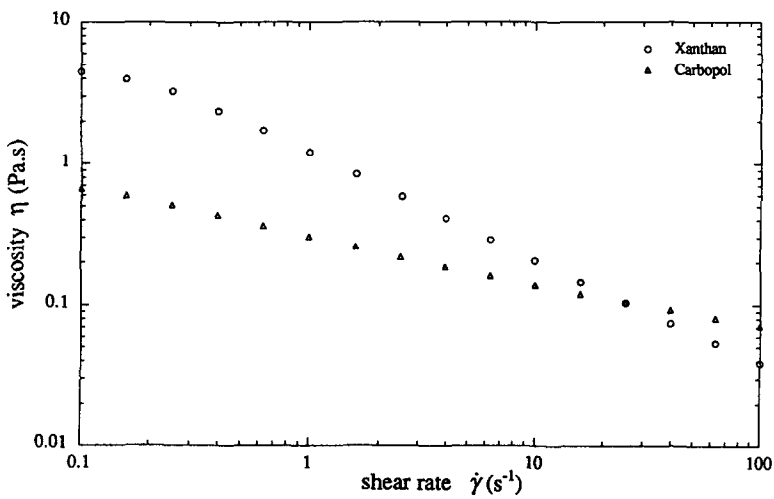

Fig. 4. The viscosities of 0.3% aqueous Xanthan and 0.4% Carbopol in 50/50 glycerin–water solution as a function of the shear rate at a temperature of 24.5°C. The Xanthan solution has a higher but more shear thinning viscosity than the Carbopol solution.

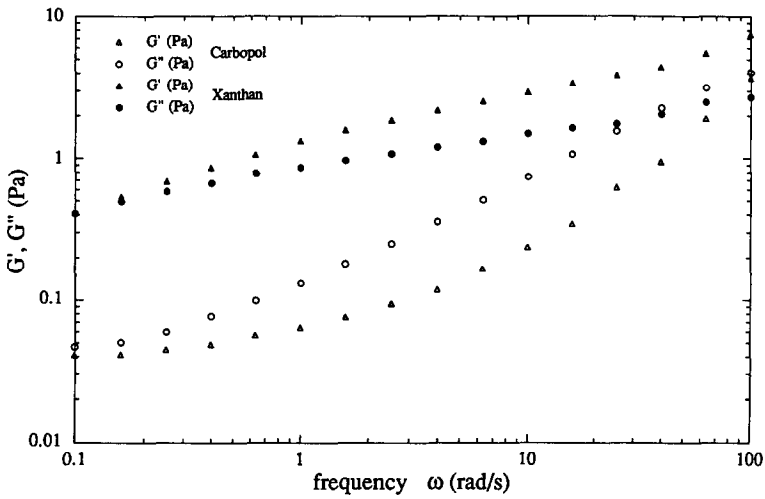

Fig. 5. Dynamic moduli of Xanthan and Carbopol solutions. In modest shear rates ranging from 0.1 to 100, both the storage modulus and loss modulus of the Xanthan solution are higher than those of the Carbopol solution. Also, in the Xanthan, the storage modulus G' is greater than the loss modulus G'', but in the Carbopol the opposite is true.

in 50/50 glycerin–water has a measurable value of the first normal stress difference, and it does not climb a rotating rod.

To determine the effects of shear thinning with a strong memory but no normal stresses, we used a solution of 0.3% Xanthan (Kelco) in water. The graph of viscosity vs shear rate is shown in Fig. 4, and the variation of the storage and loss moduli with frequency is shown in Fig. 5. This Xanthan solution is very shear thinning and it apparently has no normal stresses. We could not register a first normal stress difference on the Rheometrics fluid rheometer and the 0.3% Xanthan solution would not climb a rotating rod. On the other hand, this fluid has a high storage modulus and can be said to be linearly elastic.

3. Rolling of spheres down the side wall of a channel; experimental setup

Six different types of spheres and three channels were used in our experiments as shown in Table 2. The motion of 1/4-in diameter sedimenting spheres in the thin bed is basically two dimensional, with spheres centering themselves between two close walls. The centering was described by Liu and Joseph [11]. Close side walls have a marked effect on the magnitude of the fall velocity and rotation rate of spheres rolling down an inclined wall. But the direction of the rolling and other qualitative properties of aggregation of sedimenting spheres, sphere–wall interactions and the

TABLE 2

The channels and spheres used in our experiments for various liquids

Channel dimensions (in)	Sphere[a] material and density (g cm^{-3})					
	Plastic (1.34)	Teflon (2.18)	Rubber (5)	Steel-1 (7.61)	Steel-2 (7.61)	Tungsten (15.8)
0.275 × 4 × 23	—	glycerine	—	polyox polyacryl-amide STP glycerin	—	STP
0.85 × 0.85 × 18	Xanthan Carbopol glycerin	Xanthan Carbopol S1 glycerin	Xanthan	S1 glycerin	STP	S1
1 × 1.63 × 28	—	—	—	—	STP	—

[a] All spheres of diameter 0.25 in, except for Steel-2, 0.5 in.

tilting of long sedimenting bodies, do not depend strongly on the aspect ratio.

In this experiment, we tilted our sedimentation channel with its center plane vertical and the side walls inclined to the vertical. The angle of inclination from the vertical is θ (Fig. 6). When $\theta = 0°$, the plane of rolling is vertical. We measured the fall velocity and rolling velocity of spheres on

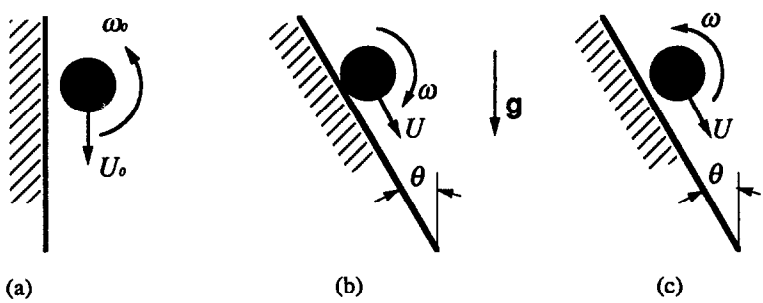

Fig. 6. Settling of spheres at the inclined wall of a channel. The inclination angle from the vertical is θ. (a) Anomalous (hydrodynamic) rolling of a sphere next to a vertical wall ($\theta = 0°$). In Newtonian liquids there is always a stand-away distance but this distance is barely visible in viscoelastic fluids because the sphere is sucked to, rather than repelled by, the wall. (b) Normal (dry) rolling is found in Newtonian liquids and in viscoelastic liquids when θ is larger than a critical value. (c) Anomalous rolling in a viscoelastic liquid. There must be a gap between the sphere and the wall, but it is usually too small to be seen at first glance. We say that a sphere slips when it falls but does not rotate.

a video system. The measurements were routine and accurate. We were unable to get an accurate measurement of the distance between the wall and the sphere in the viscoelastic case of close approach. The drag on the sphere must be strongly influenced by the precise value of this too-small-to measure stand-away distance. A more detailed study than the one undertaken here would look systematically at weight and size effects of particles. We did many casual tests of this type, but found no surprising results. Our view is that more systematic experiments should be undertaken only after some hypotheses about the controlling viscoelastic mechanisms have been formulated for testing.

The case of vertical settling ($\theta = 0°$) is special. If a sphere is initially dropped at or near a vertical wall, it will always turn counter-clockwise, as shown in Fig. 6(a), whether the fluid is viscoelastic or inelastic. We have found that spheres dropped in a viscoelastic liquid near a vertical wall are sucked to the wall, but the same spheres will move a certain distance away from the wall when they are dropped in inelastic fluids. The striking difference will be documented in another paper (Joseph et al. [13]). For now it will suffice to note once again that independently of whether the sphere migrates to the wall or takes up a small stand-off as it falls, it will turn counter-clockwise as it falls.

4. Rolling of spheres down the side wall of a channel; experimental results

We might have thought that friction emanating from the wall would turn the sphere clockwise. Evidently the small gap between the falling sphere and the wall partially blocks the fluid, so that the main flow and the main shears are on the outside of the sphere, where passage is not blocked, turning the sphere, as in Fig. 1. The sense of the rotation of the sphere, then, which has been dropped from the rest in close proximity to a vertical wall, must be anomalous, since much of the fluid cannot get through the small gap between the wall and the sphere, and instead must go around the outside. The blockage effect is greatly enhanced in viscoelastic fluids because the viscoelastic forces draw the spheres to the wall, even when the wall is vertical.

It is evident from the consideration just introduced that the fluid dynamics of sphere–wall interactions are such as to produce anomalous rolling when the relative weight of the sphere is not sufficient to hold it on the wall against countervailing hydrodynamic lift forces. This is always the case when the wall is vertical and even when θ is very small. In this sense, anomalous rolling is normal whenever hydrodynamic lift forces are at work. The lift forces are sensitive to the Reynolds number and a sphere will "fly" if the forward speed is fast enough no matter what the value of the angle of

tilt. Spheres settling on an inclined wall however need not reach the forward velocity necessary for levitation against the component of the buoyant weight of the sphere pushing it on the wall.

Our experiments using the $0.275 \times 4 \times 23$-in channel filled with pure glycerin and steel balls are representative for Newtonian liquids. When $\theta = 0°$, with vertical settling, a sphere started at the wall will be repelled by the wall and will commence to role in the anomalous sense as in Fig. 6(a). When $\theta \geq 1°$, the sphere falls to the wall and a gap is not evident; it slips at the wall ($1° < \theta \leq 4°$) or slips a lot and rolls normally a little ($4° < \theta \leq 10°$), rotates normally with a little slip ($10° < \theta \leq 30°$) or rotates normally with no slip ($\theta > 30°$).

The interval of θ for normal rolling and slipping depends on the Reynolds number and hence changes with the weight of the sphere and the aspect ratio of the channel. We carried out experiments with Teflon spheres in the narrow channel and steel and Teflon spheres in the square channel with different quantitative but the same qualitative results. We have already remarked that we expect the spheres to lift off the inclined walls at a higher Reynolds number, not seen in our experiments.

Our experiments with 0.4% Carbopol in 50/50 glycerin–water solutions were carried out in the $0.85 \times 0.85 \times 18$-in channel using plastic and Teflon balls. The wall does not attract these balls when it is vertical ($\theta = 0°$); a sphere dropped next to the wall will rotate in the anomalous way and drift away from the wall to an equilibrium stand-away distance, as in Newtonian fluids. In the case of walls with slight tilting ($0° < \theta \leq 10°$), the sphere falls to the wall, first rotating up the wall, then slipping without rolling. This behavior is intermediate between Newtonian and viscoelastic behavior, but is more nearly Newtonian.

We turn next to the experiments with viscoelastic liquids in which a vertical wall attracts rather than repels sedimenting spheres; that is, all solutions mentioned in this paper other than glycerin and Carbopol. Naturally, an inclined wall will attract a sphere more strongly than a vertical wall. The anomaly is that in these cases of sedimentation with close approach, as if touching, the sphere rotates anomalously, with "dry" rolling taking over only for relatively horizontal tilting of the wall.

In Table 3 we give the measured values of the terminal fall velocity U_0 and the terminal angular velocity ω_0. It is of interest to compare the measured values of U_0 with computed values of the Stokes velocity U_s, which is generated from the balance between buoyancy and drag

$$\Delta\rho g \tfrac{4}{3}\pi a^3 = 6\pi\eta(1)aU_s, \tag{4.1}$$

where $\Delta\rho$ is the difference in density between the solid (Table 2) and the fluid (Table 1), $g = 980\ \mathrm{cm\ s^{-1}}$, $a = 1/8$ or $1/4$-in is the sphere radius and

TABLE 3

Measured values of terminal fall speed U_0 and terminal angular velocity ω_0 of spheres falling close to a vertical wall

Liquid–solid	$\Delta\rho$ (g cm^{-3})	$\eta(1)$ (poise)	U_s (cm s^{-1})	U_0 (cm s^{-1})	U_s/U_0	$\mathbb{R}$	ω_0 (rad s^{-1})	C
1.5% polyox–steel	6.61	101	1.44	0.46	3.12	0.003	0.306	0.21
1.25% polyox–steel	6.61	64.2	2.26	1.358	1.66	0.013	0.333	0.08
1.0% polyox–steel	6.61	39.7	3.66	3.06	1.19	0.049	0.396	0.04
Xanthan–plastic	0.34	11	0.68	0.269	2.52	0.016	0.126	0.15
S1–teflon	1.3	71.4	0.40	0.656	0.61	0.005	0.167	0.08
S1–steel	6.73	71.4	2.07	1.59	1.30	0.012	0.43	0.08
S1–tungsten	14.92	71.4	4.59	4.16	1.10	0.032	0.541	0.04
STP–steel(0.25 in)	6.75	178	0.83	0.206	4.04	0.001	0.097	0.15
STP–steel (0.5 in)	6.75	178	3.33	0.708	4.70	0.004	0.133	0.12
STP–tungsten	14.94	178	1.84	0.374	4.93	0.001	0.111	0.10

The Reynolds number, $\mathbb{R} = 2a\rho U_0/\eta(1)$ where a is the radius of the sphere and $\eta(1)$ is the viscosity at shear rate 1, is small enough to assume that the computed value of the Stokes velocity U_s is relevant. $C = a\omega_0/U_0$ is the coefficient correlating U_0 and ω_0.

$\eta(1)$ $(=k)$ is the viscosity at $\dot{\gamma} = 1$ (Table 1), which we used because of uncertainty in the value of η_0. In most cases (except the one of a Teflon sphere in S1 solution), the Stokes drag is smaller than the drag in our experiments. The main reason for this discrepancy is that the nearby wall to which the sphere is attracted exerts an additional drag, as do nearby side walls. The measured value of ω_0 is corrected with the measured value of U_0 by the following argument. In dry rolling $U_0 = a\omega_0$ so that in hydrodynamic rolling, we might find a relationship like $CU_0 = a\omega_0$ with an unknown C between zero and one. Of course the sense of ω_0 is reversed in hydrodynamic rolling, and the shear from the outside is a less effective turner than dry friction.

Our experiments with 0.3% Xanthan in water were carried out in the square channel, using plastic, Teflon and rubber balls. The Xanthan solution is very interesting because it has an appreciable linear elasticity (a high storage modulus) and is very shear thinning (Table 1), yet has no measurable normal stress. A plastic sphere, which is light and settles slowly

($U_0 = 0.269\ \text{cm s}^{-1}$), is attracted to a vertical wall where it rotates anomalously with a slow angular velocity ($\omega_0 = 0.126\ \text{rad s}^{-1}$). The heavier Teflon sphere falls faster ($U_0 = 13.12$) than the shear wave speed ($c = 12.2$) and it levitates off the wall. The fall velocity for Teflon and rubber spheres is too great to determine the value of the angular velocity. In the case of a tilted wall, data were taken only for Teflon spheres. These were attracted to the wall when $\theta \leq 5°$ even though the wall repels the sphere at $\theta = 0°$. The rotation was very weak, with appreciable amounts of slipping for angles of 5, 10, 15 and 20. The weak rolling was anomalous for 5 and 10°; there was only slip at $\theta = 15°$ and slip plus normal rolling at $\theta = 20°$. The plastic sphere was attracted to the vertical and inclined walls where its rotation was too slow to measure. The rubber sphere at about $\theta = 5°$ to the wall falls and rotates anomalously, but it settles so fast that the angular velocity could not be measured accurately. It is certain that a lighter sphere would levitate at the large velocities at which the rubber spheres fell. The behavior of spheres rolling on walls in Xanthan is intermediate between Newtonian and viscoelastic, but is more nearly viscoelastic.

In our experiments using 1/4-in steel balls on the flat side wall of the narrow channel (Table 2) filled with 1.2% polyacrylamide in 50/50 aqueous glycerin, we found intermittent slipping interspersed with anomalous rolling for $0° \leq \theta < 20°$. Only slip was observed for 25 and 30° and intermittent slipping and normal rolling for $\theta = 35$, 40 and 44°. In all cases a very slight gap could be detected between the ball and the plane; the ball was hydrodynamically levitated in a position of close approach.

We did the same experiment with a 1/4-in wire laid against the flat surface. The contact between the sphere and the wire is less severe than the contact between the sphere and a flat wall. The gap under rolling on the inclined wire changes radically across the gap. There are only very small differences in the outcome of experiments using these two wall surfaces.

Now we give some measured results in graphical form for the terminal settling and angular speed of rolling spheres as functions of the angle θ of inclination of a tilted wall in aqueous Polyox, STP and S1. The settling speed U and angular speed ω are normalized by their values U_0 and ω_0 at $\theta = 0°$. In all cases, anomalous rolling is observed.

We have presented the data in two forms. First we given U/U_0 as a function of $\cos\theta$. The force driving the tangential motion of the sphere down the plane is the buoyant force $\Delta\rho g \cos\theta(4/3)\pi a^3$, linear in $\cos\theta$. For a linear response between the velocity and driving force and velocity, we might expect that $U \propto C_1 \cos\theta$ where C_1 depends on geometrical and fluid parameters and is a sort of drag coefficient. We have attempted to make a best guess at the parameter from the measured data, but the response is not rigorously linear and the fits are not convincing. In fact we really do not

expect linearity for no other reason than that the normal force exerted on the inclined plane varies with θ. This variation will produce a change in the small gap between the sphere and the plane and change the drag emanating from the wall.

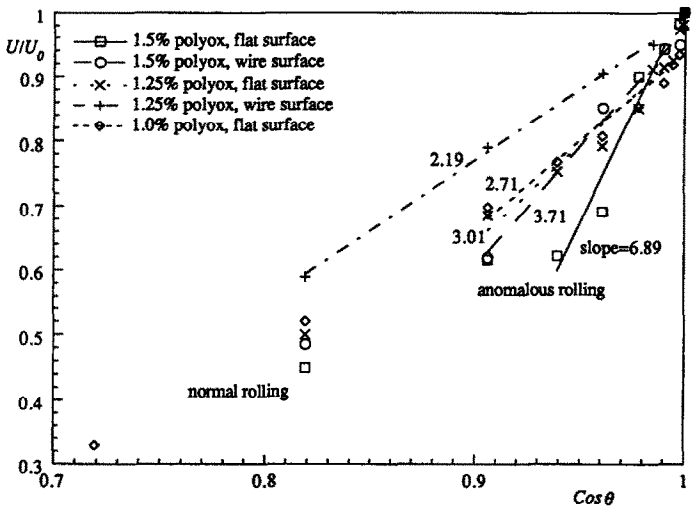

Fig. 7. Normalized fall velocity U/U_0 as a function of cos θ for a 1/4-in steel sphere falling in aqueous Polyox in the narrow channel of $0.275 \times 4 \times 23$-in. The straight lines are generated from a linear curve fitting routine using data only for anomalous rolling on an inclined wall. This fit excludes vertical settling data ($\theta = 0°$) which has no normal component of buoyant weight, and also excludes normal data from normal rolling with a too great normal component of buoyant weight.

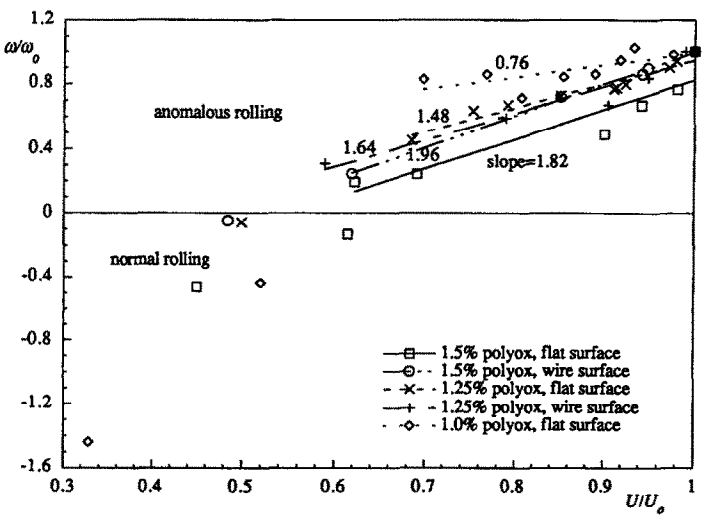

Fig. 8. Normalized angular velocity vs. normalized fall velocity for aqueous Polyox.

A second form for presenting data is as ω/ω_0 vs U/U_0. We expect to see a more or less linear relation $\omega/\omega_0 \propto C_2 U/U_0$ based on the idea that ω and U have the same dependence on $\cos\theta$, whatever that dependence might be. This idea seems to work.

In Fig. 7 and 8, we have presented results for aqueous Polyox (WSR 301) solutions. We were able to obtain reproducible data exhibiting anomalous rolling only in the more concentrated solutions: 1.5%, 1.25% and 1%. Anomalous rolling occurs in the 0.85% solution. In the 0.75% solution, results are ambiguous, with a high degree of slipping and very little rolling, behaving like Newtonian fluids. Polyox solutions of 0.6% and less exhibit only normal rolling. We are able to enhance the angular velocity of rolling in the 1.5% Polyox solution by putting a wire on the inclined wall. This effect was not so marked in the 1.25% solution.

In Fig. 9, we have presented measured values of U/U_0 vs $\cos\theta$ for S1. We drew the best straight line by linear fitting, excluding data points for dry rolling in which the sphere is not levitated and for hydrodynamic rolling in the vertical in which there is no normal gravity force. The data relating U/U_0 and ω/ω_0, in Fig. 10, fall close to a straight line satisfying $\omega/\omega_0 \propto 2.37(U/U_0)$.

In Fig. 11, we have presented measured values of U/U_0 vs $\cos\theta$ for STP in two different channels and fitted the data to straight lines $U/U_0 \propto C_1 \cos\theta$, where $C_1 = 1.37$ for the 1/4-in tungsten sphere in a

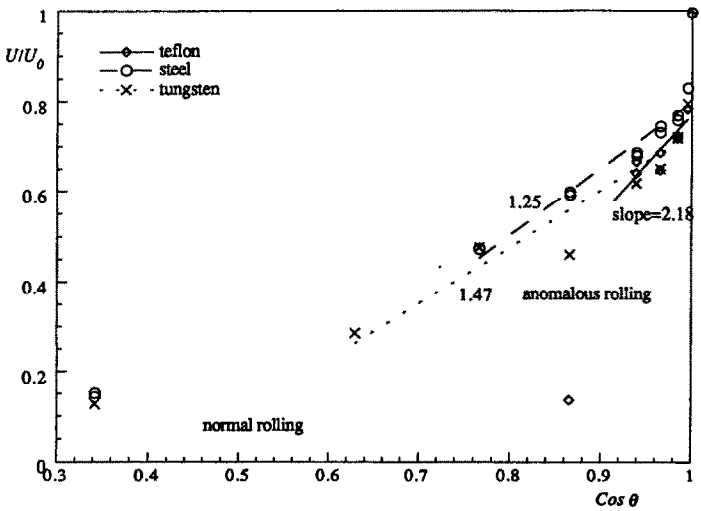

Fig. 9. Normalized fall velocity U/U_0 as a function of $\cos\theta$ for 1/4-in teflon, steel and tungsten spheres falling in S1 solution in the wide channel of 0.85 × 0.85 × 18-in. The straight lines are generated by a linear curve fitting routine from data on anomalous rolling, excluding data from normal rolling and vertical settling.

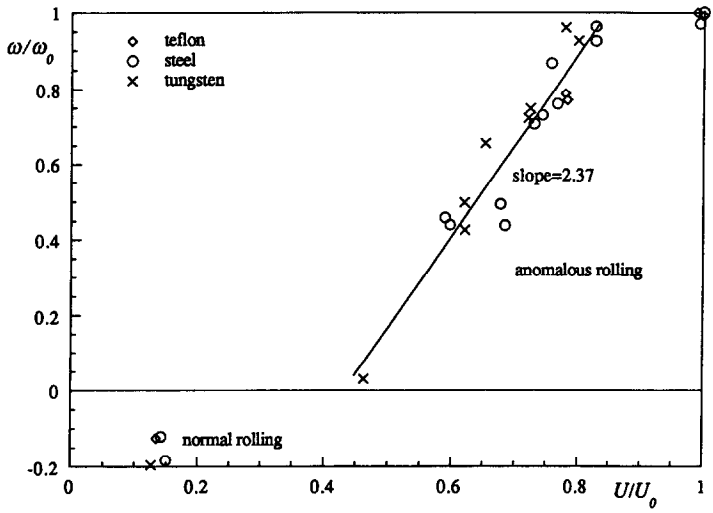

Fig. 10. Normalized angular velocity vs. normalized fall velocity for S1 solutions. Excluding data points for normal rolling and hydrodynamic rolling in the vertical, the data cluster around a straight line with slope of 2.37.

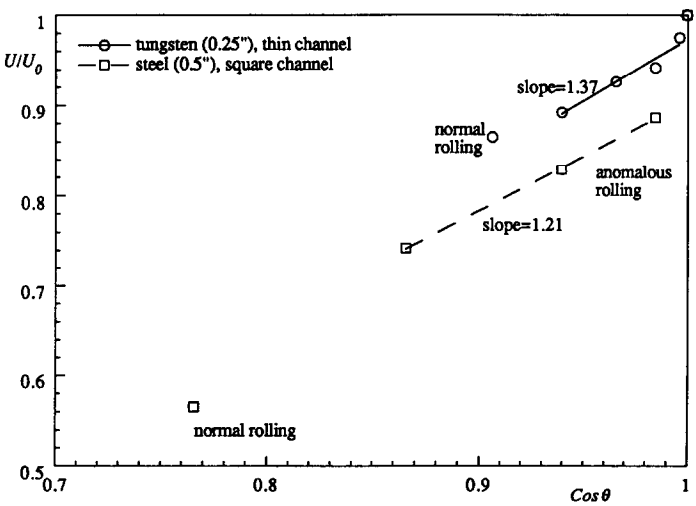

Fig. 11. Normalized fall velocity U/U_0 as a function of $\cos\theta$ for 1/4-in tungsten spheres in a $0.275 \times 4 \times 23$-in channel and 1/2-in steel spheres falling in a $0.85 \times 0.85 \times 18$-in channel filled with S1 solution.

$0.275 \times 4 \times 23$-in channel and $C_1 = 1.21$ for the 1/2-in steel ball in a $0.85 \times 0.85 \times 18$-in square channel. Straight lines $\omega/\omega_0 \propto C_2(U/U_0)$, where $C_2 = 9.58$ for a tungsten sphere and $C_2 = 2.53$ for a steel sphere, are shown in Fig. 12.

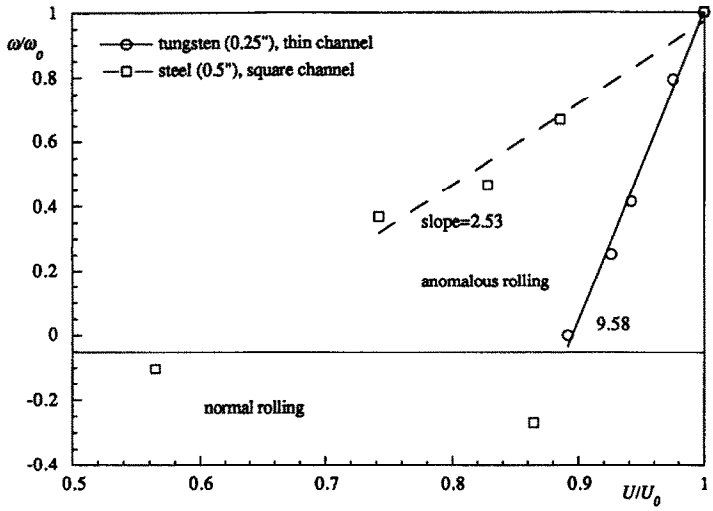

Fig. 12. Normalized angular velocity vs. normalized fall velocity for STP.

5. Direct numerical simulation of the settling of a circular particle at a vertical wall in a Newtonian fluid

The hydrodynamic mechanisms that cause circular particles to rotate and drift away from a vertical wall can be understood by direct (two-dimensional) numerical simulation, using the Navier–Stokes equations to find the fluid motion and the hydrodynamic forces that move a rigid particle according to Newton's equation of motion. A finite-element package with this capability has been presented by Hu et al. [14], and a video of this simulation together with a short paper has been given by Hu et al. [15]. Huang et al. [16] applied this code to the problem of finding the forces that control the turning couple on an elliptic particle settling in a vertical channel, and they showed that there is highe pressure on the front side of the ellipse at the place where the shear stress vanishes, which corresponds to a stagnation point in potential flow. This pressure always acts to keep the long side of the body perpendicular to the fall. Feng et al. [17] used this code to solve initial value problems for circular particles settling in a channel and this section is an adaptation of their work to the problem at hand.

We want to understand how a heavier-than-liquid, circular particle dropped from rest in this liquid at a vertical wall will rotate and move. Referring to Feng et al. [17] for details, we note here that in the regime of moderately low Reynolds numbers in which there is no vortex shedding, the particle will drift to channel center under the influence of side forces from

both walls. The problem at hand could be posed in the semi-infinite domain on the right of the vertical wall, but is here simulated by diminishing the influence of the other wall by moving it far away.

In our experiments, spheres dropped from rest in glycerin would rotate and drift rapidly away from the wall and after a short time reach an apparently steady state with a definite angular velocity ω_0 and a fixed stand-away distance with no further side drift. In the simulation, the particle is seen to drift to the center of the channel, and the drift takes place on a much larger time scale. The rotation of the particle is anomalous at the beginning, and dies away as the particle approaches its equilibrium position at the channel center (Fig. 13).

At first, when the particle is very near the wall, the passage of fluid between the circular particle and the wall is blocked, so that the flow passes over the outside of the circular particle, turning it in the direction that we called "anomalous". This is clear from the streamline around the particle as seen in a reference frame fixed on the center of the particle (Fig. 14(a)).

We are going to demonstrate that the pressure and shear stress distributions on the surface of the particle show that the maximum pressure occurs roughly at the point of vanishing modified shear stress (Fig. 15). The circular particle is rotating counter-clockwise, so that the no-slip condition implies that there are no stagnation points on the surface of the circle. In

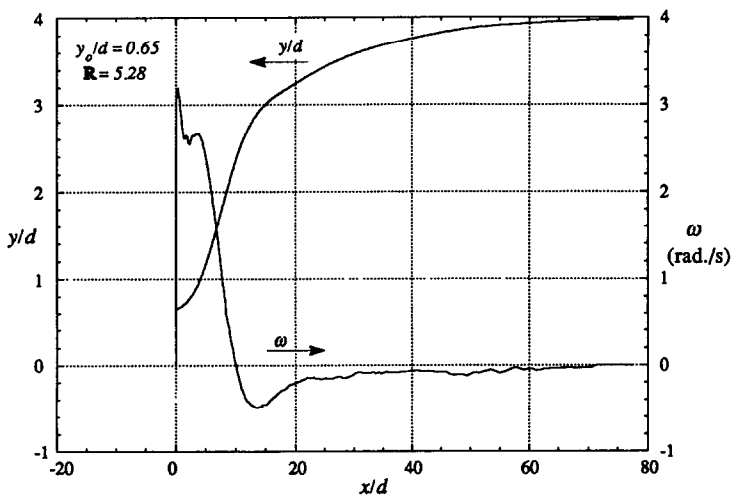

Fig. 13. Trajectory and angular velocity of a circular particle settling near a vertical wall in an 8/1 channel. The particle is released at $y_0 = 0.65d$, d being the diameter, and the final Reynolds number is $\mathbb{R} = 5.28$. The rotation of the particle is anomalous at first but gives way to normal rolling of a much smaller magnitude in the final stage of its drift to the center of the channel at $y = 4d$.

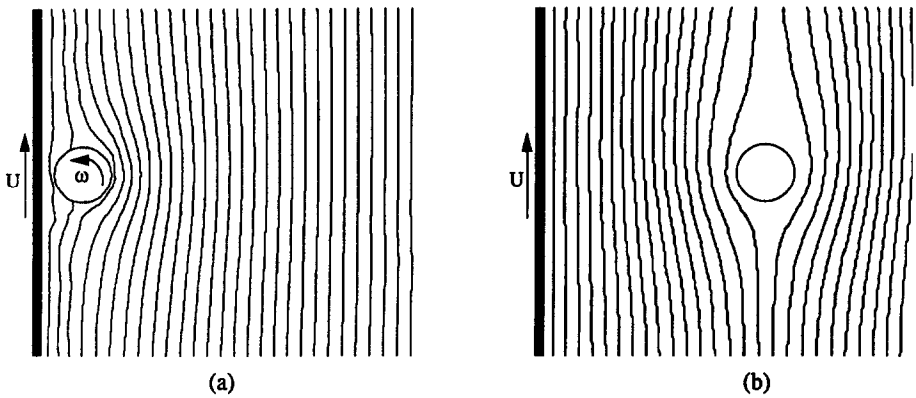

Fig. 14. Streamlines around a particle settling near a vertical wall. (a) At the start of the sedimentation (computer time step Itime = 006, $x/d = 10^{-3}$), blockage at the wall causes shift of the "stagnation points" and anomalous rolling; (b) When the particle is away from the wall, drifting and rotation of the particle die away (Itime = 280, $x/d = 76$).

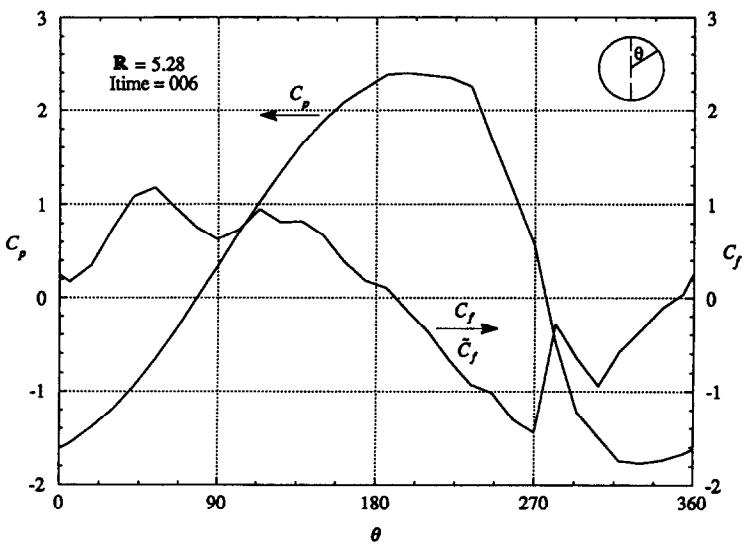

Fig. 15. Pressure and shear stress distribution on a circular particle, at $\mathbb{R} = 5.28$, in terms of dimensionless coefficients $C_p = 2p/\rho U^2$ and $C_f = 2\tau_{r\theta}/\rho U^2$ where U is the falling speed at Itime = 280 or $x/d = 76$ (see Fig. 13). The modified stress distributions $\tilde{\tau}_{r\theta}$ (5.3) is expressed through the modified coefficient $\tilde{C}_f$. Because the angular speed is small the difference between $\tilde{C}_f$ and C_f is only about 0.3% and cannot be seen in this plot. The maximum pressure is very near to the "stagnation" point where the modified shear stress vanishes ($\tilde{C}_f = 0$) on the front face of the circle.

potential flow, the fluid slips at the boundary and the rotation that is here associated with the angular velocity ω of the circle would be put in as the strength of a potential vortex with velocity

$$u_\theta^{\mathrm{p}} = \omega a^2/r. \tag{5.1}$$

The shear stress at $r = a$ for this is

$$\tau_{r\theta}^{\mathrm{p}} = -2\eta\omega. \tag{5.2}$$

The modified shear stress on the circle at $r = a$

$$\tilde{\tau}_{r\theta} \overset{\mathrm{def}}{=} \tau_{r\theta} - \tau_{r\theta}^{\mathrm{p}} \tag{5.3}$$

is "free" of the viscous effects of rotation and the zeros of $\tilde{\tau}_{r\theta}$ are a better image of the position of the effective points of stagnation, near to a streamline. This stagnation pressure in the narrow gap induces side drift away from the wall. There is a second point on the side of the circle near the wall where the shear stress vanishes, corresponding to a rear stagnation point of negative pressure, which is of smaller magnitude and not so closely associated with a zero of the shear stress.

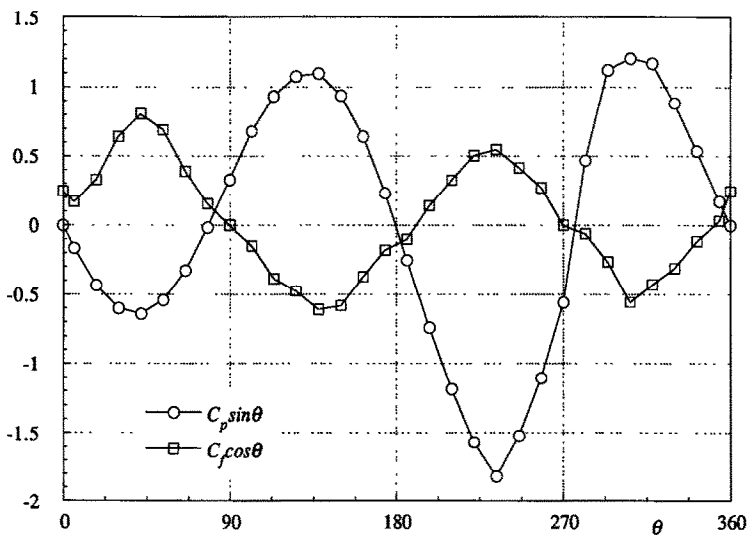

Fig. 16. Distributions of the side thrust coefficients for the pressure $C_p \sin\theta$, for the viscous part of the normal stress $C_\sigma \sin\theta$ and for the shear stress $C_f \cos\theta$ on the surface of a circular particle settling near a wall with $\mathbb{R}e = 5.28$ and $x/d = 10^{-3}$. The resultant side thrusts are given by (5.4). The lateral thrust of the pressure gives rise to the largest contribution of the total thrust. The lateral thrust of the shear stress opposes the thrust of the total normal stress due to pressure and viscosity.

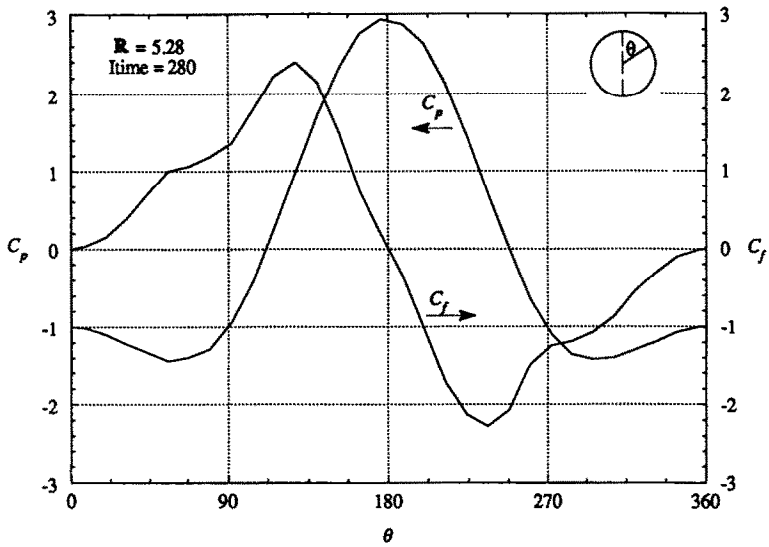

Fig. 17. Pressure and shear stress distribution on a circular particle at $\mathbb{R}e = 5.28$ and $x/d = 76$. The particle has almost stopped rotating and the maximum pressure is at the "stagnation" point $\theta = 180°$ where $C_f = 0$. Of course, pressure recovery on the rear of the circle has been greatly suppressed by viscosity.

In Fig. 16 we have compared the side thrusts, $p \sin\theta$ of the pressure and $\tau \cos\theta$ of the shear stress on the boundary $r = 0$ of the circular particle shown in Fig. 14(a). The side force resultants of these stresses are given by integration over θ

$$[F_p, F_\tau] = \int_0^{2\pi} [p \sin\theta,\ \tau \cos\theta] a \, d\theta$$

$$= [-0.062, 0.013] \text{dyne cm}^{-1}. \tag{5.4}$$

The lateral thrust of the pressure gives rise to the largest contribution to the total thrust. The lateral thrust of the shear stress opposes the thrust due to pressure and viscosity.

After the particle drifts sufficiently far away from the wall, the blockage is relieved and a more symmetrical flow pattern is achieved (Fig. 14(b)). The pressure and shear stress on the circle resemble those on a fixed particle in a uniform flow (Fig. 17), and the rotation and lateral drift eventually vanish.

6. Discussion and conclusions

We have studied the motion of a sphere falling and rotating on a plane inclined with respect to gravity. The sphere is forced toward the plane by the component of its buoyant weight normal to the plane and is moved

along the plane by the tangential component of the relative weight. If the normal component of the relevant weight is large enough, the sphere will make effective contact with the plane and will roll normally about the point of effective contact, as it does in air. The normal component may be increased by tilting the plane toward the horizontal, or by increasing the weight of the sphere.

The effects of the interaction between the moving sphere and the suspending liquid introduce countervailing forces that tend to levitate the sphere and to make it rotate in the anomalous way, opposite to what would be expected from dry rolling. The sense of rolling we have called anomalous is actually normal for the hydrodynamically levitated case, and it could be called hydrodynamic rolling, opposite to dry rolling.

There is a marked difference in the migration of spheres dropped near a vertical wall. In Newtonian liquids, dilute solutions and other solutions without strong viscoelastic properties, a sphere dropped in proximity of a vertical wall will be forced away from the wall by lift forces and be put into anomalous rotation by shears from the flow going around the outside of the sphere. We did an exact numerical simulation of this scenario for a circular particle falling near a wall in two dimensions and showed how the lateral motion of the particle and its equilibrium positions are controlled by pressures at the front and rear "stagnation" points near the wall where the shear stress vanishes.

In a strict sense, the no slip condition in a viscous fluid is not compatible with the notion of stagnation points as they appear in the theory of flows without viscosity. In the inviscid theory, stagnation points appear at dividing streamlines and a natural image of these points for a viscous fluid, say with a boundary layer, are points on the boundary at which the shear stress vanishes. We find the highest pressure at a point on the front face of the sedimenting circle near the "stagnation" point where the shear stress vanishes. There is also a point on the rear face where the shear stress vanishes, but without the pressure recovery and, in fact, the minimum pressure is very near to this point. The magnitude of the minimum pressure is relatively small, so that the outward drift of the particle is controlled by the component of the "stagnation pressure" on the front face pushing the particle away from the wall. We cannot carry our simulation into a semi-infinite regime, but in a channel, even with side walls far away, the particle will drift slowly to the center of the channel. At higher Reynolds number, after vortex shedding commences, equilibrium at off-center mean positions can be seen [17]. It is probable that slow drift away from a wall at low Reynolds number in a semi-infinite region is a permanent condition, with ever slower sidewise drifting as time goes on.

The results of the two-dimensional simulations do not give rise to the fixed stand-away distance that is observed when spheres are dropped in a Newtonian fluid near a wall. Maybe the experiments are at fault, with channel lengths too small to seen a continuous increase in the distance between the particle and the wall. Another possibility is that the theory for two dimensions is not realized in three.

The considerations of the previous paragraph do not apply to viscoelastic fluids in which particles are attracted to a wall. These include aqueous polyox in concentrations of 0.85% and higher, 0.3% aqueous Xanthan, 1.2% polyacrylamide in 50/50 glycerin–water, S1, STP and many others. In this case the conclusion is inescapable that there is a very small equilibrium distance between the wall and the particle.

The Reynolds numbers encountered in our experiments on the settling of spheres at a vertical wall in viscoelastic fluids were in most cases very small, of the order 10^{-2}. The measured value of settling speed was smaller than the values computed using Stokes formula, typically one-fifth as large (Table 3). The discrepancy is due to the wall effect produced by the small stand-away distance that seems to be required by the dynamics of wall attraction. The angular speed $a\omega_0$ of the rolling sphere is a fraction of the forward speed U_0 ranging between 0.04 and 0.21.

When the wall is tilted with respect to gravity so that the sphere falls onto the wall, the sphere will rotate normally as it does with dry friction; it will slip without rotating or it will rotate anomalously as in hydrodynamic rolling on a vertical wall. Normal rolling occurred in all the Newtonian liquids we tried, in semi-dilute aqueous polyox solutions with concentrations not greater than 0.6%, in 0.4% Carbopol solution and in all the viscoelastic fluids in which the tilt angle is greater than 20 or 30° from the vertical. Anomalous rolling or slip was observed for tilt angles less than the critical ones for normal rolling in aqueous polyox of concentration greater than 0.75%, 1.2% polyacrylamide in 50/50 glycerine–water solution, 0.3% aqueous Xanthan, S1 and STP, with a greater degree of slip for angles near to normal rolling.

We have not identified the mechanisms that produce anomalous rolling in the viscoelastic liquids mentioned at the end of the last paragraph. Liu and Joseph [11] gave an argument suggesting that viscoelasticity could change the sign of the "effective" pressure, the first normal stress at the front stagnation point. This might produce the pull required for wall–sphere attraction. Joseph and Liu [18] discussed the combined effects of shear thinning and memory in producing evanescent corridors of reduced viscosity that would promote chaining and might cause long bodies to turn their long or broad side parallel to the stream. The behavior of 0.3% aqueous Xanthan is important, because it exhibits attraction and anomalous rolling,

but only weakly. Since normal stresses in shear are absent in this liquid, we cannot conclude that large normal stresses are required. On the other hand, STP has very little shear thinning and it does exhibit the typical behavior, so that the presence of shear thinning also seems not to be required. In fact, the phenomena do not occur in the Carbopol solution which shear thins but exhibits no normal stress effects. All of the viscoelastic fluids with normal stresses show sphere–wall attraction and anomalous rolling better than 0.3% aqueous Xanthan, suggesting that the conventional measures play a more important role than strong shear thinning with a memory.

Acknowledgements

This work was supported by the NSF, fluid, particulate and hydraulic systems; by the US Army, Mathematics, and the Army High Performance Computing Research Center (AHPCRC); by the Department of Energy, Department of Basic Energy Sciences; and by the Minnesota Supercomputer Institute. We wish to thank Mr. T. Blomstrom, Mr. M. Arney and Ms. S. Braasch, who measured the rod climbing constants, surface tensions, shear wave speeds and viscosities.

References

1 A.J. Goldman, R.G. Cox and H. Brenner, Slow viscous motion of a sphere parallel to a plane wall. I. Motion through a quiescent fluid, Chem. Eng. Sci., 22 (1967) 637–651.
2 P.A. Bungay and H. Brenner, The motion of a closely-fitting sphere in a fluid-filled tube, Int. J. Multiphase Flow, 1 (1973) 25–26.
3 J.A.C. Humphrey and H. Murata, On the motion of solid spheres falling through viscous fluids in vertical and inclined tubes, ASME 1991 Winter Ann. Meeting, Paper No. WAM-91-9.
4 S.A. Dhahir and K. Walters, On non-Newtonian flow past a cylinder in a confined flow, J. Rheol., 33 (1989) 781–804.
5 D.M. Jones and K. Walters, The behavior of polymer solutions in extension-dominated flows, with applications to enhanced oil recovery, Rheol. Acta, 28 (1989) 482–498.
6 D.D. Joseph, J. Nelson, H. Hu and Y.J. Liu, Competition between inertial pressures and normal stresses in the flow induced anisotropy of solid particles, P. Moldenaers and R. Keunings (Eds.), Theoretical and Applied Rheology, Elsevier, Amsterdam, 1992, pp. 60–65.
7 G.S. Beavers and D.D. Joseph, The rotating rod viscometer, J. Fluid Mech., 69 (1975) 475–511.
8 D.D. Joseph, M.S. Arney, G. Gillberg, H. Hu, D. Hultman, C. Verdier and T.M. Vinagre, A spinning drop tensioextensiometer, J. Rheol., 36 (1992) 621–662.
9 D.D. Joseph, Fluid Dynamics of Viscoelastic Liquids, Springer-Verlag, New York, 1990.
10 R. Roscoe, The steady elongation of elasto-viscous liquids, Br. J. Appl. Phys., 16 (1965) 1567–1571.
11 Y.J. Liu and D.D. Joseph, Sedimentation of particles in polymer solutions, to appear in J. Fluid Mech., (1993) (see AHPCRC Preprint 93–032).

12 J.P. Hartnett and M. Kostic, Heat transfer to Newtonian and non-Newtonian fluids in rectangular ducts, Adv. Heat Transfer, 19 (1989) 297–354.
13 D.D. Joseph, Y.J. Liu, J. Feng, M. Poletto and J. Lin, Aggregation and dispersion of spheres falling in viscoelastic fluids, J. Non-Newtonian Fluid Mech., submitted.
14 H. Hu, D.D. Joseph and M.J. Crochet, Direct simulation of fluid particle motions, Theoret. Comput. Fluid Dyn., 3 (1992) 285–306.
15 H. Hu, D.D. Joseph and A.F. Fortes, Experiments and direct simulation of fluid particle motion, Int. Video J. Eng. Res., 2 (1992) 17–24.
16 Y. Huang, J. Feng and D.D. Joseph, The turning couples on an elliptic particle settling in a vertical channel, to appear in J. Fluid Mech. (see UMSI Research Report 93/55).
17 J. Feng, H. Hu and D.D. Joseph, Direct simulation of initial value problems for the motion of solid bodies in a Newtonian fluid. Part 1. Sedimentation, to appear in J. Fluid Mech. (see UMSI Research Report 93/60).
18 D.D. Joseph and Y.J. Liu, Orientation of long bodies falling in a viscoelastic liquid, submitted to J. Rheology (see AHPCRC Preprint 93-047).